

## Free-standing $\text{Al}_x\text{Ga}_{1-x}\text{As}$ heterostructures by gas-phase etching of germanium

Garrett D. Cole,<sup>1,a)</sup> Yu Bai,<sup>2</sup> Markus Aspelmeyer,<sup>1</sup> and Eugene A. Fitzgerald<sup>2</sup>

<sup>1</sup>Fakultät für Physik, Universität Wien, Boltzmannngasse 5, A-1090 Vienna, Austria

<sup>2</sup>Department of Materials Science and Engineering, Massachusetts Institute of Technology, Cambridge, Massachusetts 02139, USA

(Received 11 April 2010; accepted 25 May 2010; published online 28 June 2010)

We outline a facile fabrication technique for the realization of free-standing  $\text{Al}_x\text{Ga}_{1-x}\text{As}$  heterostructures of arbitrary aluminum content. Utilizing xenon difluoride ( $\text{XeF}_2$ ) we rapidly and selectively remove a sacrificial germanium (Ge) underlayer in a room temperature gas-phase etching procedure. We demonstrate two possibilities for exploiting this unique process: (1) bulk micromachining of a suspended high-frequency low-dissipation micro-optomechanical resonator consisting of an epitaxial GaAs/AlAs multilayer grown on a Ge substrate and (2) epitaxial lift-off of a GaAs film via removal of an embedded Ge sacrificial layer, resulting in lateral etch rates up to 3 mm/h and a conservative selectivity of  $\sim 10^6$ . © 2010 American Institute of Physics.

[doi:10.1063/1.3455104]

Selective etching of a sacrificial material is a fundamental technique for the realization of free-standing films for a diverse suite of applications. By propagating the etch to full release, this technique may be used to realize heterogeneous integration of disparate materials systems via epitaxial lift-off (ELO) and subsequent wafer bonding.<sup>1</sup> On the other hand, by terminating the etch at a desired undercut distance, sacrificial etching is instrumental in the construction of micro- and nanomechanical devices through the partial removal of an underlying film. Here, we present a unique lateral etch procedure utilizing  $\text{XeF}_2$  to rapidly and selectively remove a sacrificial crystalline Ge layer.

For previously demonstrated micromachining processes relevant to monocrystalline GaAs compounds (encompassing low aluminum content AlGaAs, InGaAs, InGaP, etc.), typically, a sacrificial AlAs layer is selectively removed through immersion in an aqueous hydrofluoric (HF) acid solution. This process enables rapid etch rates [up to 30 mm/h (Ref. 2)] and excellent selectivity [ $10^7$  (Ref. 3)] and has been exploited to produce high-quality free-standing heterostructures, resulting in the fabrication of numerous devices transferred to foreign substrates including high electron mobility transistors,<sup>4</sup> light emitting and laser diodes,<sup>5,6</sup> photodetectors,<sup>7</sup> and solar cells.<sup>2</sup> However, using this method, the undercut structures are inherently limited to aluminum mole fractions below 40%, due to the rapid enhancement in etch rate with increasing aluminum content in ternary  $\text{Al}_x\text{Ga}_{1-x}\text{As}$  alloys.<sup>8</sup> At the opposite extreme of alloy composition, the production of suspended high-aluminum content films may be realized via selective etching of GaAs by employing a buffered citric-acid solution, though this etchant requires a minimum of 10%–12% aluminum in the epilayers for selective etching.<sup>9</sup> Although citric-acid-based etching processes are useful for the development of small-scale suspended structures, these solutions do not exhibit the requisite selectivity for implementation in ELO.

In contrast to the aforementioned wet chemical etching processes, the technique described in this manuscript relies

on the spontaneous room-temperature reaction of a gaseous precursor, specifically the noble-gas halide,  $\text{XeF}_2$ , with Ge. Along with a rapid etch rate and high selectivity to  $\text{Al}_x\text{Ga}_{1-x}\text{As}$  alloys, further advantages of this gas-phase etchant include the elimination of surface tension forces in the release of suspended structures, and the alleviation of ion-induced damage associated with plasma exposure. Potential reaction paths for this process include the following:  $\text{Ge(s)} + 2\text{XeF}_2(\text{g}) \rightarrow 2\text{Xe(g)} + \text{GeF}_4(\text{g})$  and  $\text{Ge(s)} + \text{XeF}_2(\text{g}) \rightarrow \text{Xe(g)} + \text{GeF}_2(\text{g})$ . Although not typically considered in Si etching by  $\text{XeF}_2$  [where  $>85\%$  of etch product is  $\text{SiF}_4$  (Ref. 10)],  $\text{GeF}_2$  is included here based on the enhanced stability of the +2 oxidation state in group IV-B with increasing atomic number, as well as the experimental evidence for this species as recorded with a residual gas analyzer.<sup>11</sup> However, the involatility of the  $\text{GeF}_2$  calls into question the efficiency of this route, as the vapor pressure under the nominal process conditions is extrapolated to be  $\sim 10^{-6}$  Torr from Ref. 12. Calculations of the enthalpies of reaction for both routes yield exothermic  $\Delta H^\circ(298\text{ K})$  values of  $-976\text{ kJ/mol}$  and  $-437\text{ kJ/mol}$  of Ge, respectively; thus, self-heating effects are expected as in Si etching. For the time being, we assume that the mechanism behind spontaneous etching of Ge is analogous with that of Si.<sup>13</sup> This process proceeds via adsorption and subsequent dissociation of  $\text{XeF}_2$ , resulting in the formation of a thin surface film consisting of  $\text{GeF}_x$  lower fluorides ( $x=1-3$ ), with Xe rapidly returning to the gas phase, and the reaction terminating with the generation and desorption of a volatile product— $\text{GeF}_4$  being the most likely candidate.<sup>14</sup> Further work will be necessary to quantify the fraction of reaction products evolved in this process.

Previously, one of the authors has reported a procedure for the gas-phase etching of low-temperature deposited amorphous Ge for the construction of suspended dielectric films.<sup>15</sup> In this manuscript we build upon recent advances in the growth of III–V/Ge heterostructures<sup>16</sup> and demonstrate the feasibility of fabricating free-standing *monocrystalline* films, allowing access to a realm of solid-state systems that has had a tremendous impact in the physics and technology of semiconductors. To establish the viability of this technique

<sup>a)</sup>Electronic mail: garrett.cole@univie.ac.at.

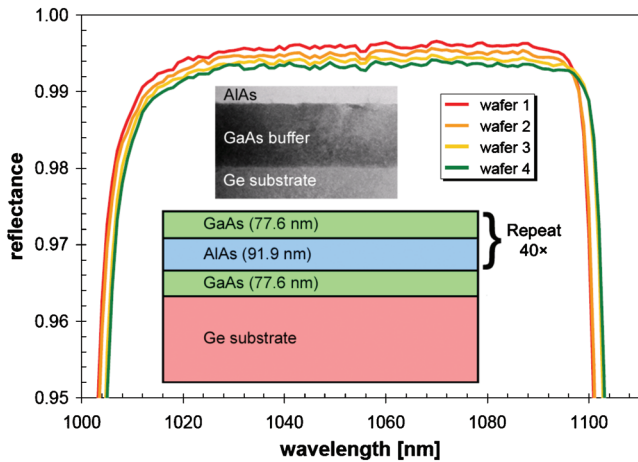


FIG. 1. (Color) On-wafer reflectance spectrum of the binary DBR as measured by spectrophotometry. Fitting these curves with a transmission matrix model yields the thickness of the epitaxial structure ( $6.67 \mu\text{m}$ ). The inset includes a cross-sectional schematic of the materials structure, as well as a TEM image of the first mirror period, revealing sharp, and defect-free interfaces.

we describe two demonstration processes: the first focuses on the development of optomechanical resonators based on a suspended binary GaAs/AlAs distributed Bragg reflector (DBR) relevant to the emerging field of quantum optomechanics;<sup>17</sup> for the second we demonstrate the lift-off of submicron epitaxial GaAs films via selective etching of a crystalline Ge sacrificial layer.

As shown in Fig. 1, the optomechanical resonators are fabricated from an epitaxial DBR consisting of 40.5 periods of alternating GaAs (high index) and AlAs (low index), grown on a 2 in. diameter,  $375 \mu\text{m}$  thick, epi-ready (100) Ge substrate, offcut  $6^\circ$  toward the [011] direction. The use of the offcut substrate is necessary to obtain high quality GaAs epitaxy on Ge by inhibiting the generation of antiphase boundaries (APBs).<sup>16</sup> The DBR is grown using a Thomas Swan/AIXTRON low-pressure metal organic chemical vapor deposition system with a close-coupled showerhead configuration. Nitrogen is used as the carrier gas and the chamber pressure is maintained at 100 Torr during crystal growth.

Postgrowth analysis of the DBR yields a surface roughness exceeding  $30 \text{ \AA}$  as measured by atomic force microscopy. We attribute this roughness to the strain field originating from defects in the epitaxial film stack, potentially arising from the interfacial misfit dislocations caused by lattice mismatch between the Ge substrate and the GaAs/AlAs multilayer; as well as the residual APBs at the Ge/GaAs interface. Scattering losses due to this excessive roughness limit the maximum theoretical amplitude reflectance to 99.87%. Further development is necessary to optimize the material quality; for example, indium and phosphorus could be incorporated in the GaAs and AlAs layers, respectively, in order to match the lattice constant of the Ge substrate and thus reduce the density of misfit dislocations.

Fabrication of the resonators entails a single-mask bulk micromachining process beginning with lithographic patterning of the device geometry. This pattern is then transferred into the epitaxial structure via an inductively coupled plasma reactive ion etch through the mirror stack using  $\text{SiCl}_4/\text{N}_2$ ,<sup>18</sup> with masking provided by the resist. Note that for these 40.5-period DBR samples, the vertical etch depth approaches  $7 \mu\text{m}$ . An overetching time of approximately 20% is utilized

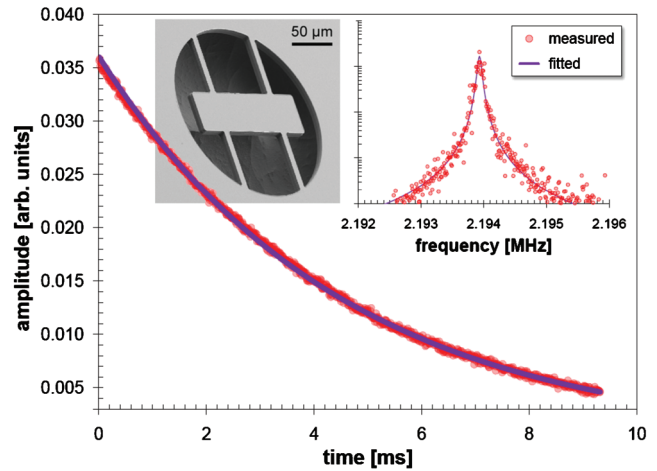


FIG. 2. (Color) Micrograph and measured free-ringdown response of a completed optomechanical resonator. As shown in the inset spectral plot, this device has a free-free resonance near 2.2 MHz, resulting in a quality factor of  $3.18 \times 10^4$  at 20 K in vacuum.

to eliminate footing at the base of the DBR. To complete the processing of the resonators, the masking resist is stripped and the devices are undercut in a pulsed  $\text{XeF}_2$  etching system.<sup>19</sup> Each etching pulse runs for 30 s with 4 Torr of  $\text{XeF}_2$  and 6 Torr of  $\text{N}_2$ ; between each etch cycle the chamber is evacuated and a fresh charge of  $\text{XeF}_2$  is introduced. A micrograph highlighting a completed resonator is included in Fig. 2; the details of the mechanical design of these devices may be found in Ref. 20. Through a reduction in anchor loss, we observe a significant increase in the quality factor for these structures (up to  $5.1 \times 10^4$  at 2.1 MHz) as compared with our initial epitaxial devices.<sup>9</sup>

Measurements of the Ge etch rate are carried out using a combination of stylus profilometry and dual-beam scanning electron microscopy/focused ion beam milling. We record a vertical etch distance of  $60 \mu\text{m}$  into the Ge substrate, realized in ten cycles of 30 s long  $\text{XeF}_2$  exposures, with no crystallographic dependence on the etch direction. Neglecting any initiation steps, this process results in a vertical etch rate of approximately  $12 \mu\text{m}/\text{min}$ . This rate is slower than that previously observed for crystalline Ge in the study of  $\text{XeF}_2$  etching in the SiGe alloy system;<sup>21</sup> but is comparable with the maximum achievable rates found in sacrificial silicon etching. The lateral etch distance under these high-pressure conditions is measured to be  $27 \mu\text{m}$ , resulting in a vertical to lateral etch rate ratio of 1.97:1. It is interesting to note that a recent investigation of high-pressure  $\text{XeF}_2$  etching of single-crystal silicon shows the opposite dependence—with more rapid in-plane etching—yielding a vertical to lateral etch ratio of 0.7:1.<sup>22</sup>

In order to explore the limits of the  $\text{XeF}_2$ -Ge etching process, we demonstrate ELO of submicron thickness, single-crystal GaAs films. Two distinct epitaxial materials structures are used in this experiment; both structures employ an epi-ready (100) GaAs substrate offcut  $6^\circ$  toward the [011] direction, followed by 190 nm of unintentionally doped (uid) Ge ( $1 \mu\text{m}$  in the second sample), capped with 180 nm (or 320 nm) of uid GaAs. Prior to etching,  $10 \times 10 \text{ mm}^2$  chips are cleaved from the original 2 in. diameter wafers and a simple rinse is performed to remove the water-soluble native oxide layer from the exposed Ge. The parameters used in our gas-phase ELO process are the same as those de-

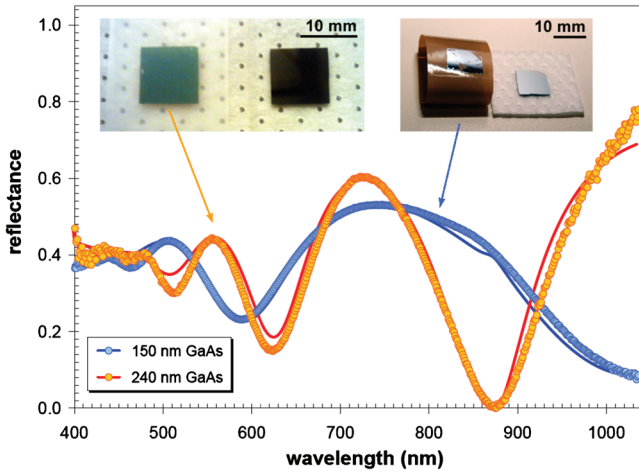


FIG. 3. (Color) Measured reflectance spectra (discrete points) of transferred GaAs films following XeF<sub>2</sub>-based ELO. Theoretical curves (solid lines) are generated using a transmission matrix model of a GaAs layer on an adhesive backing. The inset includes photographs of the epilayers and their original substrates.

scribed in the resonator process flow. Summing the total etching time, the 190-nm-thick Ge sacrificial layer is removed after 170 min; thus, we record a conservative lateral etch rate of approximately 30  $\mu\text{m}/\text{min}$  for this sample. Further tests with the 1- $\mu\text{m}$ -thick Ge layer result in an enhanced rate approaching 50  $\mu\text{m}/\text{min}$ ; a factor of 5 larger than those typically found with Si. In contrast to ion-assisted fluorocarbon etching of Si, it has been postulated that Ge etching is mediated mainly via spontaneous reaction with adsorbed fluorine.<sup>23</sup> The enhanced rates observed here confirm this mechanism and may be explained by the lower average bond strength in Ge (2.77 eV) when compared with Si (3.38 eV), as well as a decreased activation energy for GeF<sub>x</sub> product formation.<sup>23</sup> Reflectance spectra for the transferred GaAs films are shown in Fig. 3.

Transmission electron microscopy reveals as-grown GaAs film thicknesses of approximately 170 nm and 275 nm, respectively, for the ELO samples. Using the fitted reflectance data in Fig. 3, the conservative GaAs etch rate is  $1.94 \times 10^{-4}$   $\mu\text{m}/\text{min}$  and a selectivity of  $0.26 \times 10^6$  is calculated. In a second test, high-resolution electron micrographs of the DBR cross-section following 3 h of XeF<sub>2</sub> exposure show no change in thickness for the 78-nm-thick GaAs surface layer, yielding a selectivity of  $1.8 \times 10^6$  (assuming 5 nm resolution for the images). Thus, we conclude that the selectivity for this process is  $\sim 10^6$ . The lack of appreciable etching is verified by a previous study of fluorine adsorption on GaAs, where the stability of GaF<sub>3</sub> (boiling point  $\approx 1000$  °C) was found to frustrate etching.<sup>24</sup> Compared with early results for HF-based ELO [etch rate of 0.3 mm/h (Ref. 2)], the lateral etch rate for our demonstration gas-phase XeF<sub>2</sub> process shows similar selectivity, is an order of magnitude faster, and additionally enables the release of epitaxial films with arbitrary aluminum content.

We have developed a unique gas-phase underetching process based on the noble-gas halide XeF<sub>2</sub> for the fabrication of high-quality free-standing single-crystal Al<sub>x</sub>Ga<sub>1-x</sub>As structures of arbitrary aluminum content. Using this procedure we demonstrate MHz optomechanical resonators, as

well as transferred epilayers via ELO. The XeF<sub>2</sub>-based ELO technique described here is uniquely applicable for the development of substrate transferred photovoltaic structures, for example, in the lift-off of record-high-efficiency inverted cell designs that do not rely on a Ge junction.<sup>25</sup> As shown here, this process could be exploited in a variety of ways: either through the incorporation of a Ge sacrificial film on a GaAs substrate beneath the active epitaxial layers, or as a substrate removal procedure assuming the cell structure is originally grown on a Ge handle wafer. Further work will be necessary in order to identify any Ge lattice-matched compound semiconductor alloys that exhibit a spontaneous chemical reaction with XeF<sub>2</sub>.

G.D.C. is a recipient of a Marie Curie Fellowship of the European Commission (EC). Additional financial support is provided by the EC (projects MINOS, IQOS), Austrian Science Fund (projects START, L426), and the European Research Council (ERC StG QOM). Microfabrication was carried out at the Zentrum für Mikro- und Nanostrukturen (ZMNS) of the Technische Universität Wien.

- <sup>1</sup>M. Konagai, M. Sugimoto, and T. Takahashi, *J. Cryst. Growth* **45**, 277 (1978).
- <sup>2</sup>J. J. Schermer, G. J. Bauhuis, P. Mulder, E. J. Haverkamp, J. van Deelen, A. T. J. van Niftrik, and P. K. Larsen, *Thin Solid Films* **511–512**, 645 (2006).
- <sup>3</sup>E. Yablonovitch, T. Gmitter, J. P. Harbison, and R. Bhat, *Appl. Phys. Lett.* **51**, 2222 (1987).
- <sup>4</sup>D. R. Myers, J. F. Klem, and J. A. Lott, Tech. Dig. - Int. Electron Devices Meet. **1988**, 704.
- <sup>5</sup>E. Yablonovitch, E. Kapon, T. J. Gmitter, C. P. Yun, and R. Bhat, *IEEE Photonics Technol. Lett.* **1**, 41 (1989).
- <sup>6</sup>I. Pollentier, P. Demeester, A. Ackaert, L. Buydens, P. V. Daele, and R. Baets, *Electron. Lett.* **26**, 193 (1990).
- <sup>7</sup>A. Yi-Yan and W. K. Chan, *IEEE Circuits Devices Mag.* **8**, 26 (1992).
- <sup>8</sup>X. S. Wu, L. A. Coldren, and J. L. Merz, *Electron. Lett.* **21**, 558 (1985).
- <sup>9</sup>G. D. Cole, S. Gröblacher, K. Gugler, S. Gigan, and M. Aspelmeyer, *Appl. Phys. Lett.* **92**, 261108 (2008).
- <sup>10</sup>H. F. Winters and F. A. Houle, *J. Appl. Phys.* **54**, 1218 (1983).
- <sup>11</sup>J. J. Neumann, Xactix, personal communication (29 April 2010).
- <sup>12</sup>K. F. Zmbov, J. W. Hastie, R. Hauge, and J. L. Margrave, *Inorg. Chem.* **7**, 608 (1968).
- <sup>13</sup>H. F. Winters and J. W. Coburn, *Appl. Phys. Lett.* **34**, 70 (1979).
- <sup>14</sup>A. Campo, Ch. Cardinaud, and G. Turban, *J. Vac. Sci. Technol. B* **13**, 235 (1995).
- <sup>15</sup>G. D. Cole, E. Behymer, L. L. Goddard, and T. C. Bond, *J. Vac. Sci. Technol. B* **26**, 593 (2008).
- <sup>16</sup>S. M. Ting and E. A. Fitzgerald, *J. Appl. Phys.* **87**, 2618 (2000).
- <sup>17</sup>T. J. Kippenberg and K. J. Vahala, *Science* **321**, 1172 (2008).
- <sup>18</sup>S. Schartner, S. Golka, C. Pflügl, W. Schrenk, and G. Strasser, *Microelectron. Eng.* **83**, 1163 (2006).
- <sup>19</sup>Xetch e1, Xactix Inc., Pittsburgh, PA, USA.
- <sup>20</sup>G. D. Cole, I. Wilson-Rae, M. R. Vanner, S. Gröblacher, J. Pohl, M. Zorn, M. Weyers, A. Peters, and M. Aspelmeyer, IEEE 23rd International Conference on Microelectromechanical Systems (MEMS), Hong Kong, China, 24–28 Jan., 2010, pp. 847–850.
- <sup>21</sup>G. Xuan, T. N. Adam, P.-C. Lv, N. Sustersic, M. J. Copping, J. Kolodzey, J. Suehle, and E. Fitzgerald, *J. Vac. Sci. Technol. A* **26**, 385 (2008).
- <sup>22</sup>C. Easter and C. B. O'Neal, *J. Microelectromech. Syst.* **18**, 1054 (2009).
- <sup>23</sup>G. S. Oehrlein, T. D. Bestwick, P. L. Jones, M. A. Jaso, and J. L. Lindström, *J. Electrochem. Soc.* **138**, 1443 (1991).
- <sup>24</sup>W. C. Simpson and J. A. Yarmoff, *Annu. Rev. Phys. Chem.* **47**, 527 (1996).
- <sup>25</sup>J. F. Geisz, D. J. Friedman, J. S. Ward, A. Duda, W. J. Olavarria, T. E. Moriarty, J. T. Kiehl, M. J. Romero, A. G. Norman, and K. M. Jones, *Appl. Phys. Lett.* **93**, 123505 (2008).